Laser Ablation Depth Profiling of Helium in Accessory Minerals: Imaging Alpha Ejection Zones and Natural Helium Diffusional Loss Profiles

Matthijs C. van Soest, Michelle Aigner*, Kip V. Hodges, and Alexandra Pye

Group 18 Laboratories, School of Earth and Space Exploration, Arizona State University, Tempe, AZ, USA. matthijs.vansoest@asu.edu

ASU School of Earth and Space Exploration, Arizona State University

GROUP 18 LABORATORIES, ASU Center for Innovation in Isotope Chronology

Introduction

The Ultraviolet Laser Ablation Microprobe (UVLAMP) method of releasing helium from samples has so far mostly been utilized for some form of Laser Ablation (U-Th-Sm)/He dating (LAHe) or combined LAHe and Laser Ablation U-Th/Pb double dating (LADD) (e.g. 1, 2, 3, 4, 5, 6, 7). Other applications using UVLAMP have focused on 2D-mapping of helium distributions within zircon crystals (8) and stepwise Laser Ablation Depth Profiling (LADP) of induced helium diffusional loss profiles in apatite and zircon (9, 10).

Based on these successes, the stepwise helium LADP method would appear to be an excellent method to study the distribution of He within a crystal without the need for bulk heating. Thus, it avoids issues of within-experiment radiation damage annealing, diffusional flattening of helium zonation, and/or the sudden release of helium from fluid and/or melt inclusions..

In this contribution we focus on the results of high spatial resolution helium LADP experiments in a variety of accessory minerals (apatite, zircon, monazite, and titanite). The experiments are intended to a) empirically determine the alpha ejection distance and how those results compare to the distance for each mineral derived from SRIM calculations (11, 12) and b) image natural helium distribution profiles from rim to core in, with associated U, Th, and Sm depth profiles that can be equivalent to the He distribution profiles from the $^4He/^3He$ thermochronology (13) approach.

Methodology

He profiles are ablated stepwise using a Teledyne Analyte Excite Excimer laser ablation system using mineral and spot size specific predetermined ablation rates.

He released from each step is analyzed on a Noblesse mass spectrometer.

Pit depths were determined using a micro-XAM white light interferometric microscope.

Profiles were corrected for 'laser-loss' (9) using correction factors determined from depth profiles ablated, using the exact same laser settings, into large mineral slabs with generally homogeneous He distribution.

U, Th, and Sm depth profiles were analyzed using a Teledyne Analyte G2 Excimer laser with a HelEx II ablation cell attached to a Thermo iCap Qc ICP-MS.

Spots were ablated adjacent to the He LADP pits to generally the same depths.

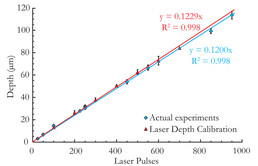

Drill rate calibration for a 100 µm round spot in Durango apatite compared to pit depths from actual LADP experiments. Drill rates are mineral and spot size specific. The depth calibration is linear to depths of >100 µm.

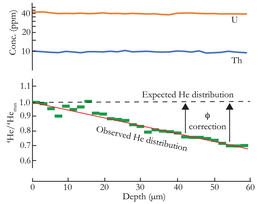

The down hole laser loss effect demonstrated with this He LADP in a large Tanzania zircon internal slab. Homogeneity of He is expected based on the homogeneous U and Th distribution in the slab.

Samples

The samples used for depth profiling are listed in the table below. Main selection criteria for this exercise was the availability of suitable grains with at least one clearly recognizable pristine crystal surface in addition to some basic knowledge about the thermal history of the sample.

Sample Name	Age (Ma)		Cooling Rate	Step	Drill Rate	Depth	αejection	zoning
	He	U-Pb		(µm)	(µm)	(µm)	zone	
Apatite;expected α stopping distance: ~21.65µm:								
Durango	31.7	31.7	Fast	3	3.1	31	Yes	No
Bitterroot Mtns.	~33.1	58.14	Intermediate	2	1.8	90.4	No	Minor
Titanite; expected α stopping distance: ~20.65µm:								
Fish Canyon	28.3	28.3	Fast	2	2.3	69.6	Yes	Minor
Karakoram Gr.	~8.1	42.0	Fast	2	2.3	92.9	Possibly	Yes
Monazite; expected α stopping distance: ~18.8µm								
Bitterroot M. 01	~38.2	58.14	Intermediate	1	0.94	28.3	Yes	Yes
Bitterroot M. 03	~38.2	58.14	Intermediate	1	0.94	28.2	Possibly	Yes
Zircon; expected α stopping distance: ~15.9µm:								
Lyon Mtn. Gr.	~100-350	~1050	Slow	2	2.1	31.0	Yes	Yes
McClure Mtn.	~5.3-520	~523.5	Slow	2	2.6	77.2	No	Yes
Fish Canyon	28.3	28.3	Fast	2	1.9	58.4	Possibly	Yes
Bitterroot Mtns.	~37.3	58.14	Intermediate	2	1.9	58.2	Possibly	Yes
E. Antarc. Mtns.	~64-96	492.4	Slow	2	2.0	91.8	No	Yes

He Depth Profiles showing evidence of zoning and diffusional loss

The following plots show He depth profiles and associated U-Th-Sm depth profiles that do not show clear evidence of an α-ejection zone, but instead show clear evidence for zoning and, in one case, for He diffusional loss.

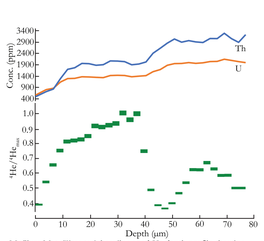

McClure Mtn. Zircon: A heavily zoned He depth profile showing some relationship to the adjacent U-Th profile and what may be the vestiges of an α-ejection zone.

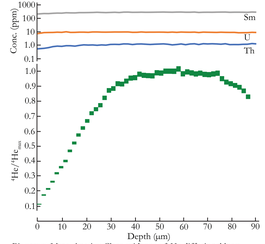

Bitterroot Mtns. Apatite: Clear evidence of He diffusional loss: gradually increasing He beyond the α-ejection zone to the core of the grain with no noticable zoning of U, Th, and Sm.

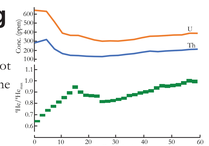

Fish Canyon Tuff Zircon: A zoned depth profile showing an apparent α-ejection zone.

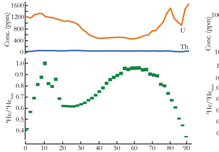

East Antarctic Mountains Zircon: A complexly zoned He depth profile.

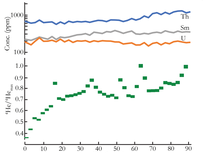

Karakoram Granodiorite Titanite: A zoned He depth profile with the vestiges of an α-ejection zone.

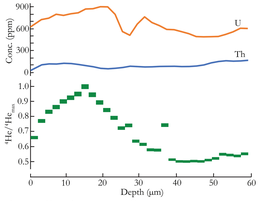

Bitterroot Mtns. Zircon: A zoned He profile with an apparent α-ejection zone.

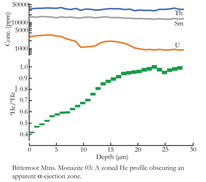

Bitterroot Mtns. Monazite 03: A zoned He profile obscuring an apparent α-ejection zone.

Depth Profiles with α-ejection zones

Here the four depth profiles that yielded unambiguous α-ejection profiles are presented together with the α-ejection distance derived from the data using a simple Monte Carlo model. Boxes represent the individual He step analyses with step-width in the x direction and normalized He compared to the maximum He encountered in any step with the box height representing the ±2σ error. When available LA-ICP-MS traces of U, Th, and Sm laser ablation depth profiling are plotted above the He depth profile. Typically these kind of analyses have an error on the order of 10% 2σ.

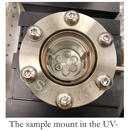

The sample mount in the UV-laser chamber.

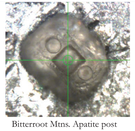

Bitterroot Mtns. Apatite post ablation.

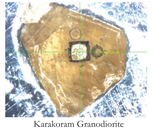

Karakoram Granodiorite Titanite post ablation.

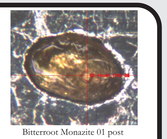

Bitterroot Monazite 01 post ablation.

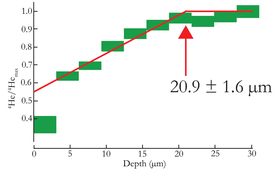

Durango Apatite, modeled α-ejection distance: 20.9 ± 1.6 µm. The boxes represent weighted mean averages of 4 different depth profiles into different faces of a large crystal.

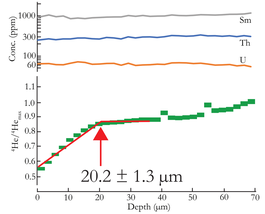

Fish Canyon Tuff Titanite, modeled α-ejection distance: 20.2 ± 1.3 µm.

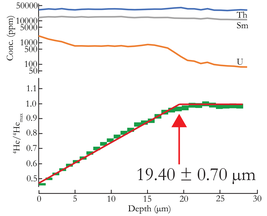

Bitterroot Mtns. Monazite 01, modeled α-ejection distance: 19.40 ± 0.70 µm. The high Th content appears to overwhelm any major effects from the obvious zoning in U.

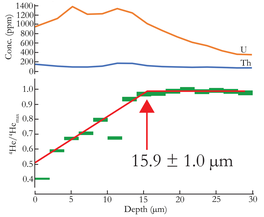

Lyon Mountain Granite Zircon, modeled α-ejection distance: 15.9 ± 1.0 µm The U and Th zoning does not appear to have affected the He distribution in the margin of the crystal.

Conclusions

1. The He LADP results show that α-ejection zones are encountered in some mineral grains and are within error of the theoretical values as established by SRIM model (11,12) calculations.

2. In many cases the He depth profiles showed clearer evidence of He zoning in response to U, Th, and in some cases possibly Sm zoning, while showing the vestiges of what could be an α-ejection zone. In one case (Bitterroot Mtns. Apatite), the profile showed clear evidence of He diffusive loss given minimal evidence for U-Th-Sm zoning.

3. Complex He zoning profiles were encountered in some tests, especially in zircon. Given the complexity internal U and Th zoning in most natural zircons, this does not come as a surprise. It implies that the application of a FT correction assuming a homogeneous distribution of U and Th or a simple zoning pattern likely explains much overdispersion in zircon (U-Th)/He datasets.

4. He LADP, in combination with LA-ICP-MS depth profiling of the mineral composition, is a highly effective tool to investigate intracrystalline He and parent isotope compositions and improve sample interpretation.

References: 1 Boyce et al. GCA 70, 2006; 2 Vermeesch et al. GCA 79, 2012; 3 Tripathy-Lang et al. JGR-ES 118, 2013; 4 Evans et al. JAAS 30, 2015; 5 Horne et al. GCA 178, 2016; 6 Horne et al. CG 506, 2019; 7 Pickering et al. GG 348, 2020; 8 Danisik et al. Sci Adv 3, 2017; 9 Van Soest et al. GCA 75, 2011; 10 Anderson et al. GCA 274, 2020; 11 Ziegler and Biersack, 1985; Ketcham et al. GCA 75, 2011; 13 Shuster and Farley EPSL 217, 2004.

Acknowledgements: Chris McDonald is acknowledged for his help producing the box depth profile plots of the He LADP data. Brian Monteleone and Jeremy Boyce are acknowledged for their help with the early long ago efforts to He LADP α-ejection zones.